JOURNAL OF MATERIALS SCIENCE **37** (2002) 2061 – 2070

Piezoelectric properties of collagen-nanocrystalline hydroxyapatite composites

C. C. SILVA
Departamento de Quimica Orgânica e Inorgânica, UFC

A. G. PINHEIRO
Laboratório de Óptica não Linear e Ciência dos Materiais (LONLCM), Departamento de Física, Universidade Federal do Ceará, Caixa Postal 6030, CEP 60455-760, Fortaleza, Ceará, Brasil

S. D. FIGUEIRÓ
Departamento de Bioquímica e Biologia Molecular Centro de Ciências, UFC, Fortaleza, Ceará, Brasil

J. C. GÓES
Departamento de Engenharia Mecânica, Centro de Tecnologia, UFC, Fortaleza, Ceará, Brasil

J. M. SASAKI, M. A. R. MIRANDA, A. S. B. SOMBRA
Laboratório de Óptica não Linear e Ciência dos Materiais (LONLCM), Departamento de Física, Universidade Federal do Ceará, Caixa Postal 6030, CEP 60455-760, Fortaleza, Ceará, Brasil
E-mail: sombra@ufc.br

In this paper we did a study of the physicochemical, dielectric and piezoelectric properties of anionic collagen and collagen-hydroxyapatite (HA) composites, considering the development of new biomaterials which have potential applications in support for cellular growth and in systems for bone regeneration. The piezoelectric strain tensor element d_{14}, the elastic constant s_{55}, and the dielectric permittivity ε_{11} were measured for the anionic collagen and collagen-HA films. For the collagen-HA composite film (Col-HACOM) the main peaks associated to the crystalline HA is present. For the nanocrystalline composite, nanometric HA powder (103 nm particle size) (HAN), obtained by mechanical milling were used. For the composite film (Col-HAN) the HA and $CaH(PO_4)_2H_2O$ phases were detected. One can see that the HA powder (HAN) present the main peaks associated to crystalline HA. The IR spectroscopy measurements on HA-COM and HAN powders, Col-HACOM and Col-HAN composite films and collagen film (Col) presents the main resonances associated to the modes of $(PO_4)^{3-}$, $(CO_3)^{2-}$. The IR spectra of Collagen Film (Col) shows the bands associated to amide I (C=O), amide II (N–H) and amide III (C–N) vibrational modes. The scanning electron photomicrography of the Col-HACOM and Col-HAN films, respectively, shows deposits of HA on the surface of collagen. It also shows that HACOM crystals has a dense feature, whereas the HAN crystals has soft porous surface. Energy-dispersive spectroscopy (EDS) analysis showed that the main elements of the hybrid sponge were carbon, oxygen, calcium, and phosphorus. The EDS of HACOM crystal, present in the Col-HACOM composite showed a molar ratio Ca/P = 1.71, whereas the Col-HAN composite the molar ratio of calcium and phosphorus (Ca/P = 2.14) and the amount of carbon were greater. The piezoelectric strain tensor element d_{14} obtained for the anionic collagen was around 0.102 pC/N. The collagen composite with nanocrystalline HA crystals (Col-HAN) present a better result ($d_{14} = 0.040$ pC/N) compared to the composite with the commercial ceramic ($d_{14} = 0.012$ pC/N). This is an indication that the nanometric particles of HA present little disturbance on the organization of the collagen fibers in the composite. In this situation the nanometric HA are the best candidates in future applications of these composites.

1. Introduction

Calcium phosphate based bioceramics, mainly in the form of hydroxyapatite (HA), have been in use in medicine and dentistry for the last 20 years. Applications include coatings of orthopedic and dental implants, alveolar ridge augmentation, maxillofacial surgery, otolaryngology, and scaffolds for bone growth and as powders in total hip and knee surgery [1]. These materials exhibit several problems of handling and fabrication, which can be overcome by mixing with a suitable binder. Recently, a great interest has been focused on the use of composites of biodegradable or bioreabsorbable materials, such as collagen [2, 3], gelatin [4], and synthetic polymers, like polyhema [5].

Collagen, which exists in a variety of morphological forms [6], is the most abundant structural protein of the animal connective tissue and has a long history as biomaterial [7]. Individual molecules of collagen, which are semi flexible rods ∼280 nm in length and ∼1 nm in diameter, undergo self-assembly to form interwoven network-like structures, ranging from long fibrils to complex structures. The native fibrils possess a high degree of axial alignment of collagen molecules and are characterized by a regular stagger of approximately 1/4 of a rod length between each molecule and its axially aligned neighbor, which is characterized by a banding pattern with a ∼67 nm period [8, 9]. In vitro, fibrils with the characteristic 67 nm pattern similar to that of the native fibril have been produced.

Some biological materials and biopolymers are found to exhibit the polar uniaxial orientation of molecular dipoles in their structure and can be considered as bioelectret. Such materials show pyroelectricity and piezoelectricity. Biocompatible polymeric materials are now used extensively after proper polarization treatment for biomedical applications such as antithrombogenic surfaces and artificial membranes [10]. Pyro and piezoelectric studies in various types of biological systems showed the presence of natural polarity in the structure of various parts of animals and plants. In many natural structures the polar molecules such as proteins are aligned in parallel with a preferred direction of the polar axis to form the crystalline structure. Therefore, such structures can be regarded as natural electrets. Because of this intrinsic polarization, pyroelectricity and piezoelectricity in the axial direction can be observed [10].

The piezoelectric properties of collagen has been investigated in complex biological systems such as bone and tendon. The piezoelectric properties of bone are of interest in view of their role in bone remodeling [11]. The stress generated potential of bone promoted osteogenesis, which are mediated by electrical current generated by piezoelectric materials through changing pressure [12]. The magnitude of the piezoelectric sensitivity coefficients of bone depends on frequency, on direction of load, and on relative humidity [13]. Values up 0.7 pC/N have been observed in bone [14]. Marino *et al.* [15] examined the relation between collagen's film piezoelectricity and its electron microscopic appearance, in films with different degree of organization, and suggest that the piezoelectric effect originate either at the level of tropocollagen.

In the present investigation, a collagen film and two composite filmes of collagen-hydroxyapatite were prepared and characterized by infrared absorption, scanning electron microscopy, X-ray diffraction, dielectric and piezoelectric investigation, considering the development of new biomaterials which have potential applications in guided bone regeneration. The first composite was prepared with the anionic collagen and a commercial hydroxyapatite (Col-HACOM) and the second one was prepared using nanocrystalline hydroxiapatite obtained by our group using mechanical alloying (Col-HAN) [16].

2. Experimental methods

2.1. Collagen preparation

The collagen was prepared by solubilization of collagen from bovine serosa after 72 h of treatment under alkaline conditions in presence of salts, followed by homogenization in acetic acid solution, at pH 3.5 [17]. The samples were dialised against acetic acid solution, at pH 3.5, and brought to a final concentration of 1%, determined by hydroxiproline [17].

2.2. HA nanocrystalline powder

In this paper mechanical alloying has been used successfully to produce nanocrystalline powders of hydroxyapatite (HA) using the procedure [16]:

$$10Ca(OH)_2 + 3P_2O_5 \xrightarrow{\text{IMPACTS}} Ca_{10}(PO_4)_6(OH)_2 + 9H_2O$$

2.2.1. Reaction 1

Commercial oxides $Ca(OH)_2$ (Vetec, 97% with 3% of $CaCO_3$), P_2O_5 (Vetec, 99%), were used in the HA preparation [16]. For this reaction the material was ground on a Fritsch Pulverisette 6 planetary mill with the stechiometric proportionality between the oxides given in above equation. Milling was performed in sealed stainless steel vials and balls under air, with 350 rpm as rotation speed. The powder mass to the ball mass ratio used in all the experiments was near 1/6. To avoid excessive heat the milling was performed in 30 min milling steps with 10 min pauses. Mechanical alloying was performed for 60 hours of milling.

To compare the efficiency of the milling process we also use Commercial Hydroxyapatite (Vetec, 98%) (HA-COM) to compare with the milled ceramics.

2.3. Preparation of the films

The composite film was casted in acrylic molds from a collagen sponge which is soaked in saturated solution of HA, and dried in laminar flow of air. The collagen sponge was prepared equilibrating the soluble collagen in phosphate buffer, 0.13 mol/L, pH 7.4 by 120 h, followed by centrifugation (10000 rpm, 1 h). The resulting gel was poured on the acrylic mold and then was lyophilized.

2.4. X-ray diffraction

The X-ray diffraction (XRD) patterns were obtained at room temperature (300 K) by step scanning using

powdered samples. We used five seconds for each step of counting time, with a Cu-K_α tube at 40 kV and 25 mA using the geometry of Bragg-Brentano. The analysis of the grain size (L_c) of the HA phase has been done for all samples using the Scherrer's equation [18],

$$L_c = \frac{k\lambda}{\beta \cos\theta}$$

where k is the shape coefficient (value between 0.9 and 1.0), λ is the wave length, β is the full width at half maximum (FWHM) of each phase and θ is the diffraction angle. For this purpose, we chose the single peak near 25.8 degree within the pattern and according to $P6_3/m$ space group of HAP, this peak correspond to $hkl = 002$, along to the **c** crystallographic axis. We have used the LaB_6 (SRM 660-National Institute of Standard Technology) powder standard pattern to determine the instrumental width ($w_{inst} = 0.087^\circ$) and afterward to calculate the crystalline size via Equation 1. The β parameter has to be correct using the following equation:

$$\beta = \sqrt{w_{exp}^2 - w_{inst}^2}$$

where w_{exp} correspond to experimental FWHM obtained for each sample. The crystalline size for the milled ceramic was obtained, assuming coefficient $k = 1$, can be seen in Fig. 3 (HAN). The XRD patterns indicates that the grain size is around 103 nm for the milled ceramic (Fig. 3, HAN) through reaction 1.

2.5. Scanning electron microscopy

The photomicrograph of membranes of collagen, and collagen-HA composite, casted in phosphate buffer pH 7.4 under 0.15 mol/L of ionic strength, were obtained on a Scanning Electron Microscope, Phillips XL-30, operating with bunches of primary electrons ranging from 12 to 20 keV, in rectangular lyophilized samples, covered with a layer of carbon of 30 nm of thickness.

2.6. Infrared spectroscopy

Transmission IR spectra were taken in a SHIMATZU FTIR-283B spectrophotometer in the wavenumber region 400–4000 cm^{-1}.

2.7. Piezoelectric and dielectric measurements

The piezoelectric and dielectric measurements were obtained from a HP 4291A Material Impedance Analyzer in conjunction with a HP 4194 Impedance Analyzer, which jointly cover the region of 100 Hz to 1.8 GHz. In Fig. 1 one has the sample geometry we used for the dielectric and piezoelectric measurements. Rectangular coordinates are assigned to the samples as shown in Fig. 1. The 2-3 plane is the sample plane, and the 1 axis is perpendicular to the plane of the sample. The flat faces of the samples are painted with a silver electrode.

3. Piezoelectric model

The piezoelectric model was already discussed in the literature [17]. The piezoelectric strain element d_{14} for

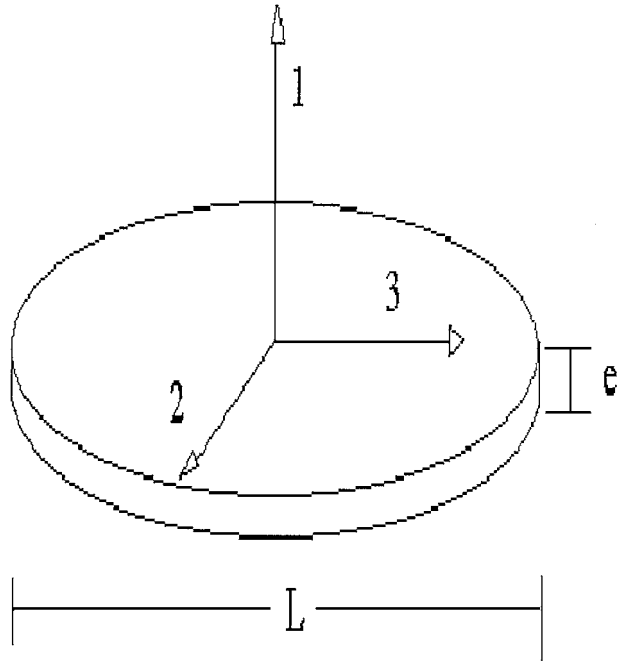

Figure 1 A rectangular coordinate assigned to the sample for the measurement of piezoelectric and dielectric constant.

the shear piezoelectric is given by [17]:

$$d_{14} = k_{14}\sqrt{\varepsilon_{11}^T s_{55}^E} \quad (1)$$

where is given by:

$$\frac{s_{55}^D}{s_{55}^E} = \frac{\varepsilon_{11}^S}{\varepsilon_{11}^T} = 1 - k_{14}^2 \quad (2)$$

Where k_{14} is the piezoelectric coupling factor, ε_{11}^T is the dielectric permittivity obtained by a measurement of the capacitance at a frequency below the fundamental resonance, ε_{11}^S is obtained by measurement of the capacitance at a frequency above the resonance mode and the elastic compliance s_{55}^D is given by:

$$s_{55}^D = \frac{1}{4\rho(f \cdot L)^2} \quad (3)$$

which is determined from the successive resonance frequencies of the shear mode. Where $f \cdot L$ is the frequency constant which is the product of the resonance frequency and the diameter of the sample (controlling dimension of the sample, $L \gg$ e, see Fig. 1) and ρ is the sample density. From the experimental measurement of ε_{11}^T, ε_{11}^S, $f \cdot L$ and ρ one can obtain s_{55}^D (Equation 3), k_{14} (Equation 2) and d_{14} (Equation 1). In Table I one has the experimental values of these constants under study [17].

3.1. Loss factor measurement

For the ceramics that are used as transducers for the generation of ultrasonic waves, considerable heat is generated in the transducer at a high power level, and thus limits the maximum radiated power. The origin of this effect has been investigated by some authors. Some of them attributed it to the dielectric hysteresis [19, 20], but its main cause was interpreted as the internal friction

TABLE I Density (ρ), thickness (e), dielectric permittivity (ε), frequency constant ($f \cdot L$) and piezoelectricity (d_{14}) of collagen and collagen-HA samples

Films	ρ (Kg/m^3)	e (μm)	1 MHz $\varepsilon_{11}^T/\varepsilon_0$	1 GHz $\varepsilon_{11}^S/\varepsilon_0$	$f \cdot L$ (kHz $\cdot$ m)	d_{14} (10^{-12} CN^{-1})
Col	948.4	27.88	1.53	1.29	253.86	0.102
Col-HACOM	930	150.72	1.89	1.87	654.22	0.012
Col-HAN	918.9	97.68	2.00	1.70	744.53	0.040

of the ceramic [19, 20]. The dissipation of mechanical energy near the resonance must be represented by an internal resistance. For the piezoelectric ceramics the internal friction and dielectric loss are found to be mostly caused by dissipation within the grain crystallite, and the major contribution of the dissipation in the grain may be the average in some sense, involving mechanical and dielectric loss losses of single domain crystal. The loss factor was measured Q^{-1} using the electric admittance resonance curve by:

$$Q^{-1} = \frac{f_2 - f_1}{f_0} \tag{4}$$

The frequencies corresponding to $|Y| = |Y_m|$ 0.707 are indicated by f_2 and f_1 where $|Y_m|$ is the peak value of the resonance and f_0 is the frequency of the resonance.

4. Results and discussion

Anionic collagen is a collagen with net negative charge in neutral pH which can be prepared by selective hydrolysis of carboxidiamides groups of residues of asparagine and glutamine present in the protein, due to alkaline treatament [21]. The biocompatibility and biodegradation studies of anionic collagen membranes showed that: cell alterations, mineralization or contact necrosis were not observed in any of the membranes studied [22]. Other work describes the preparation and characterization of anionic collagen composites with rhamsan and vinylidene fluoride-trifluorethylene with improved rheological and dielectric properties without loss of collagen secondary structure with an interaction occurring between both macromolecules of the composites [23].

4.1. X-ray diffraction

Figs 2 and 3 shows X-ray diffraction patterns of HA powders and collagen films. In Fig. 2 one has the x-ray diffraction of the commercial HA powder (HA-COM), used to prepare our first composite film, together with the x-ray diffraction from the pure collagen film and the x-ray of the composite film (Col-HACOM). In the same figure we also have the diffraction intensities of the HA and $CaHPO_4$ phases obtained from the literature (from JCPDS [24]) and denoted by bars. One can see that the HA powder (HA-COM) present the main peaks associated to crystalline HA. If one compares with the HA-REF one can notice that extra peaks are present (X) indicating that one can have an extra phase in the commercial product. This phase was identified as $CaHPO_4$. We believe that the presence of $CaHPO_4$ could be a trace of the original product of the original reaction used to produce HA.

In the same figure one has the x-ray diffraction associated to the collagen film (Col). For the collagen

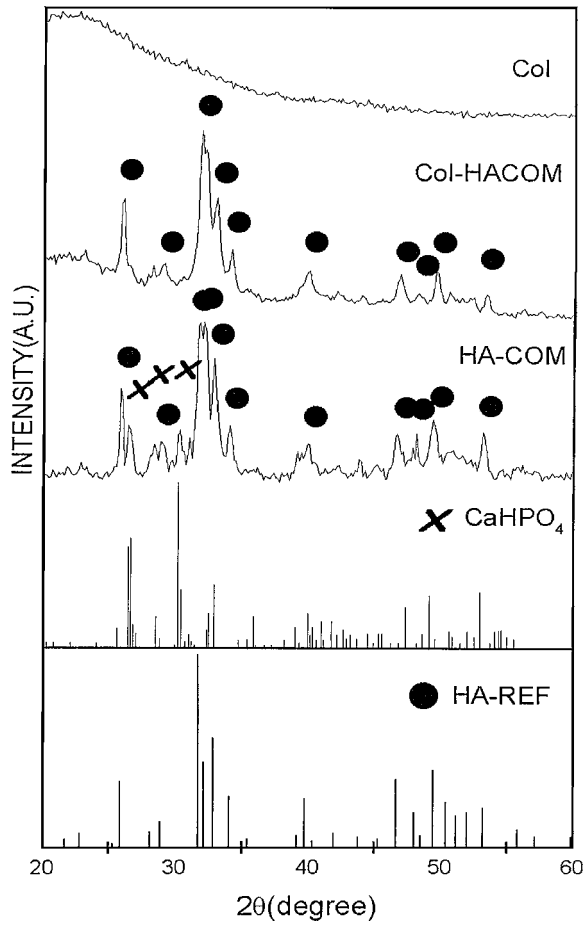

Figure 2 X-Ray diffraction of the collagen film, collagen-HACOM film, and HACOM powder. The vertical bars are associated to $CaHPO_4$ and HA obtained from the literature (JCPDS [26]).

film a broad band for the x-ray diffraction was observed (Fig. 2). For the collagen-HA composite film (Col-HACOM) a high degree of crystallization was observed. The main peaks associated to the crystalline HA is present in sample of collagen-HACOM (see Fig. 2). In Fig. 3 one has the x-ray diffraction of the nanocrystalline HA powder (HAN), obtained by mechanical milling. The process was described before. In this procedure one uses reaction 1 with 60 hours of milling. According with the x-ray diffraction the average dimension of the HA grains is around 39 nm (see Fig. 3) which were used to prepare our composite film (Col-HAN). In the same figure one has the x-ray diffraction from the pure collagen film (Col) and the x-ray of the composite film (Col-HAN). In the same figure we also have the diffraction intensities of the HA and $CaH(PO_4)_2$ H_2O phases obtained from the literature (from JCPDS [24]) and denoted by bars. One can see that the HA powder (HAN) present the main peaks associated to crystalline HA. However when we look for the composite sample (Col-HAN) one can notice peaks associated to HA

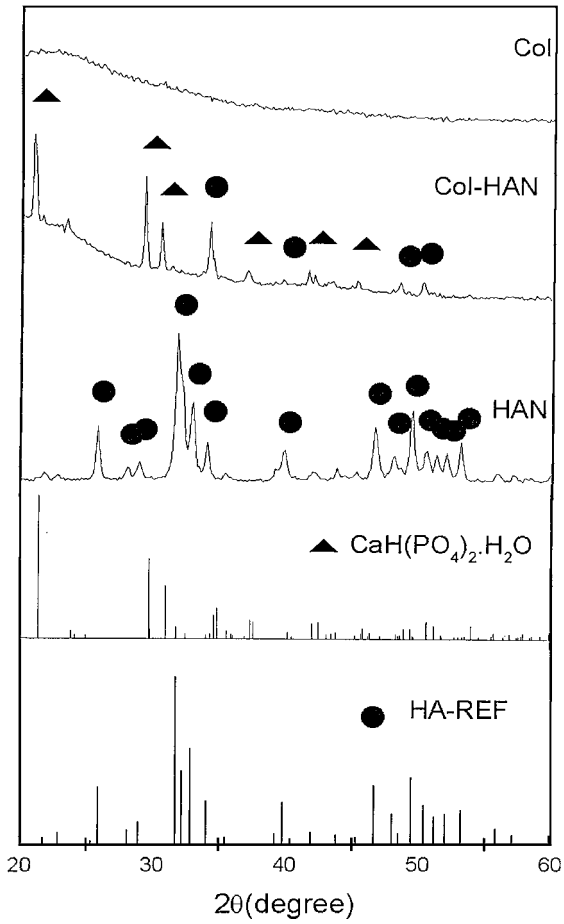

Figure 3 X-Ray diffraction of the collagen film, collagen-HAN film, and HAN powder. The vertical bars are associated to $CaH(PO_4)_2H_2O$ and HA obtained from the literature (JCPDS [26]).

and extra peaks are present (▲) indicating the presence of an extra (Ca, P) phase in the film. This phase was identified as $CaH(PO_4)_2$ H_2O. In the same figure one has the x-ray diffraction associated to the collagen film (Col). For the collagen film a broad band for the x-ray diffraction was observed (Fig. 3).

4.2. Infrared spectroscopy

In Fig. 4 one has the FT-IR spectroscopy measurements on HA-COM powder, col-HACOM composite film and collagen film (Col). For the HA-COM powder, resonances associated to the stretching mode of $(PO_4)^{3-}$ ion, were observed at 1020 and 954 cm^{-1}, respectively. Resonances associated to the stretching mode of the $(CO_3)^{2-}$ ion, were also observed at 876 cm^{-1}. The peaks at 566 and 603 cm^{-1} belong to the vibrations (ν_4) of the phosphate group of HA.

The resonances around 1445 cm^{-1} and 1420 cm^{-1} are the result of carbonate stretching vibrations. The IR spectra of Collagen Film (Col) shows a strong absorption band associated to amide I (C=O) at about 1650 cm^{-1}, a strong amide II (N–H) at 1558 cm^{-1} and a band centered at 1238 cm^{-1}, representing the amide III (C–N) vibrational modes. The ratio between absorption peaks to bands in 1238 cm^{-1} and at 1450 cm^{-1}, which has been shown to be very sensitive to the presence of the tertiary structure of native collagen, that is related to pyrrolidine ring vibrations, was always higher than one, showing that the integrity of collagen structure was maintained [25–28]. The spectrum of Col-HACOM composite sample is characterized by absorption bands arising from HA and Col, determined by analogy with FT-IR spectra of pure HA and Col standard samples. Absorption bands at 561–609 cm^{-1} associated to the $(PO_4)^{3-}$ groups of HA, while two pronounced absorption bands with maxima at 960 and 1085 cm^{-1} arise also from the phosphate groups from HA. In Fig. 5 one has the FT-IR spectroscopy measurements on HAN powder, col-HAN composite film and collagen film (Col). In this spectra, the characteristic absorption bands of HA are observed. The bands at 567 cm^{-1} (ν_4), 603 cm^{-1} (ν_4), 1041 cm^{-1} (ν_3), can be attributed to the PO_4^{3-} ion. The bands at 1473 cm^{-1} and 1413 cm^{-1} attributed to CO_3^{2-}. Vibrations associated to OH^- are detected by the band at 1630 cm^{-1}. One interesting point is the existence of absorptions associated to CO_3^{2-} at 1473 cm^{-1} and 1413 cm^{-1} for HAN. For reaction 1, HA1, one should not have the presence of Carbon, however the commercial calcium oxide ($Ca(OH)_2$) used present a level of purity around 97%, where $CaCO_3$ is present as an impurity around 3%. The spectrum of Col-HAN composite sample is

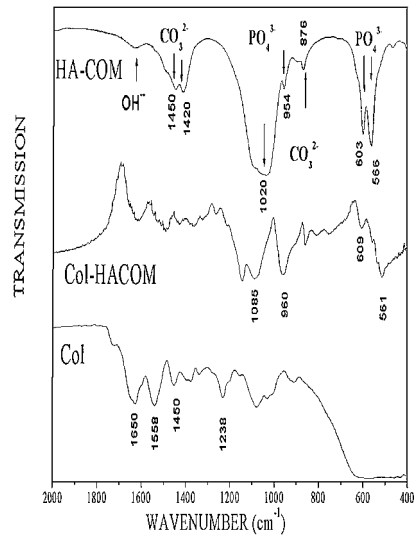

Figure 4 Infrared spectra of the collagen film, collagen-HACOM film, and HACOM powder.

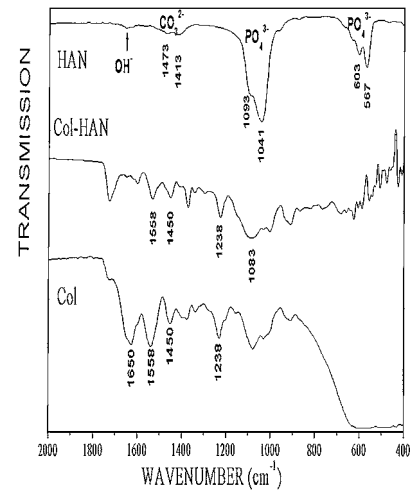

Figure 5 Infrared spectra of the collagen film, collagen-HAN film, and HAN powder.

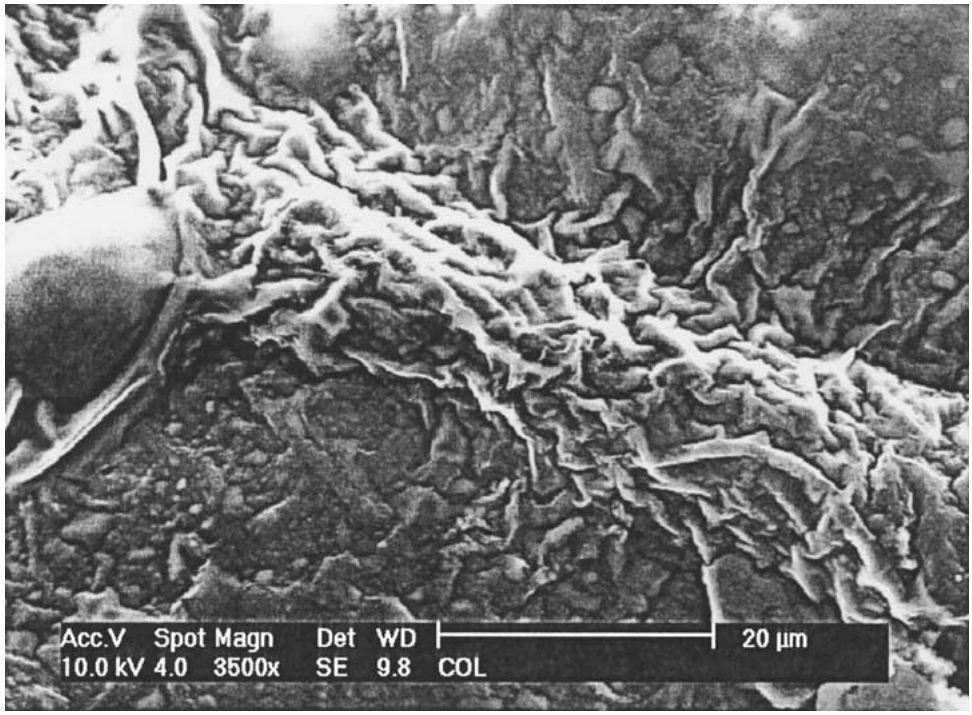

(A)

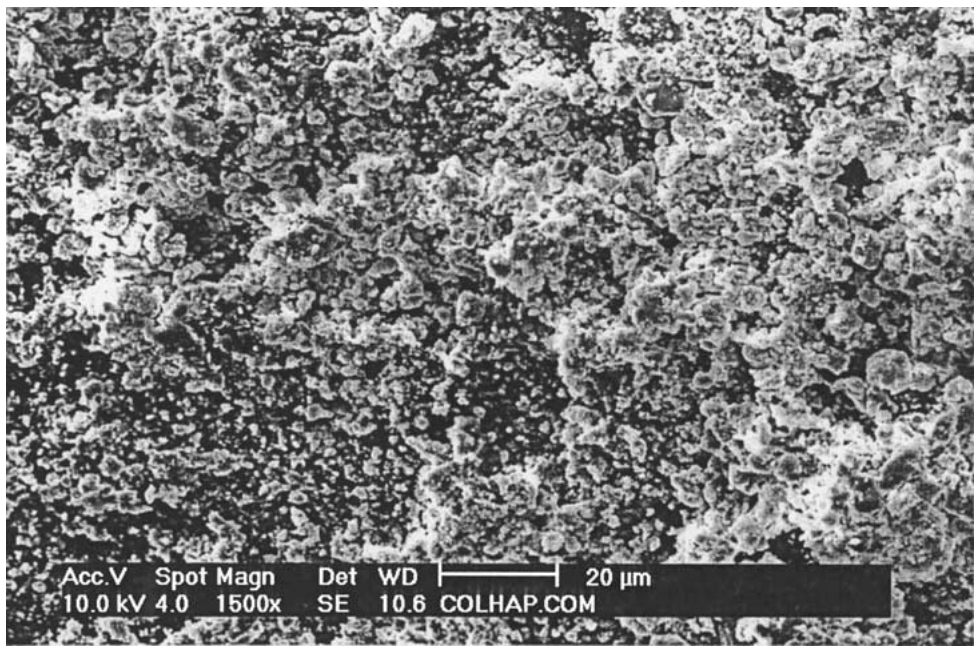

(B)

Figure 6 (A) Scanning electron photomicrograph of the anionic collagen film (3500X); (B) Scanning electron photomicrograph of the anionic collagen-HACOM composite film (1500X); (C) Scanning electron photomicrograph of the anionic collagen-HAN composite film (1500X); (D) Scanning electron photomicrograph of the anionic collagen-HACOM composite film (3500X); (E) Scanning electron photomicrograph of the anionic collagen-HAN composite film (15000X). (*Continued*).

characterized by absorption bands arising from HA and Col, determined by analogy with FT-IR spectra of pure HA and Col standard samples. Absorption bands at 561–609 cm^{-1} associated to the $(PO_4)^{3-}$ groups of HA are much weaker now, while a pronounced absorption band with maxima at 1083 cm^{-1} arise also from the phosphate groups from HA. Absorptions at 1238 cm^{-1}, 1450 cm^{-1} and 1558 cm^{-1} are associated to collagen.

4.3. Scanning electron microscopy

Fig. 6A show the scanning electron photomicrograph of anionic collagen sponge, where we can see the bundles of collagen. These fibers were soaked in a saturated solution of HA, and then dried in a laminar flow of air. Figs 6B and C show the scanning electron photomicrography of the Col-HACOM and Col-HAN films, respectively, which shows deposits of HA on the surface of collagen. Figs 6D and E shows the scanning electron photomicrography of the same films, with a higher approximation of HA crystals. It shows that HACOM crystals has a dense feature (see Fig. 6D), whereas the HAN crystals has soft porous surface (see Fig. 6E). Energy-dispersive spectroscopy (EDS) analysis (Fig. 7) showed that the main elements

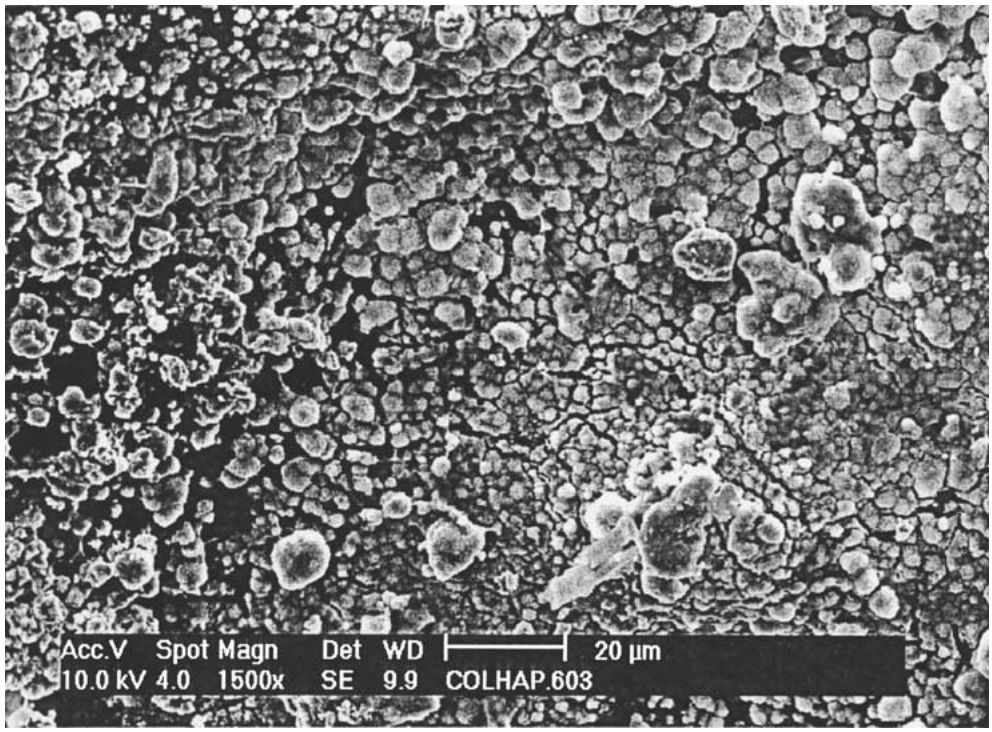

(C)

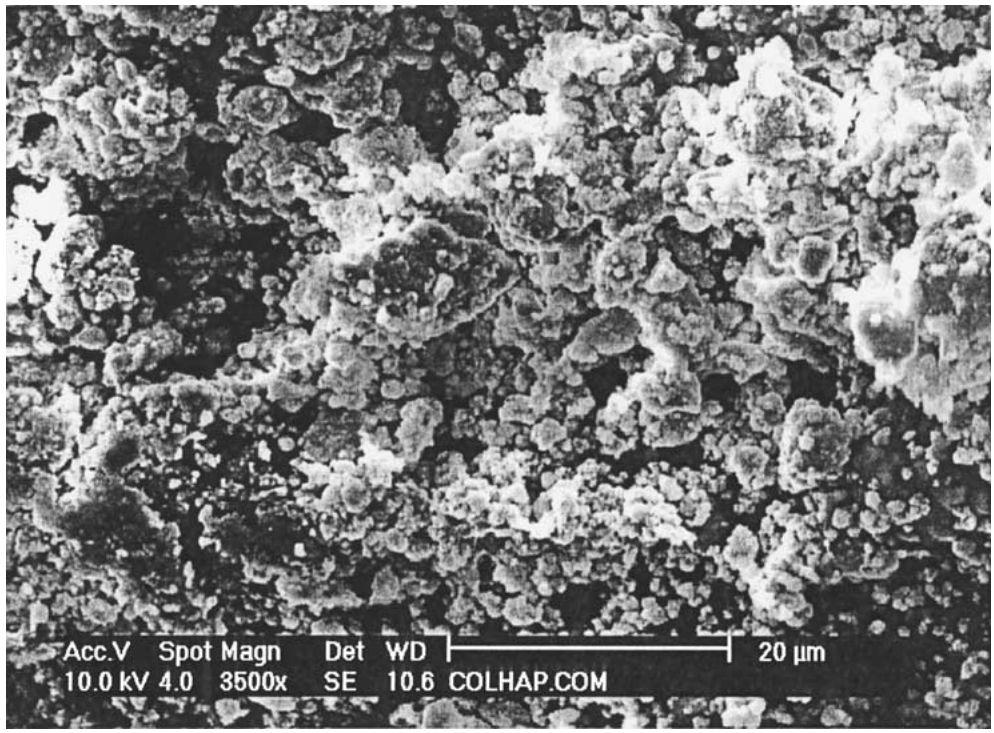

(D)

Figure 6 (*Continued*).

of the hybrid sponge were carbon, oxygen, calcium, and phosphorus. The EDS of HACOM crystal, present in the Col-HACOM composite showed a molar ratio Ca/P = 1.71 (Fig. 7), whereas the Col-HAN composite (Fig. 7) the molar ratio of calcium and phosphorus (Ca/P = 2.14) and the amount of carbon were greater. The molar ratio obatained for the pure ceramics were 2.38 for HACOM ceramic and 2.07 for the nanocrystalline ceramic (HAN, see Fig. 7). These results suggest that the HAN crystals are closer to the expected value for the ratio Ca/P for hydroxyapoatite, which is around 2.15. The HAN ceramics interact with collagen forming a composite that could be mimics the bone.

4.4. Piezoelectric measurements

In Fig. 1 one has the sample geometry we used for the dielectric and piezoelectric measurements. Rectangular coordinates are assigned to the samples as shown in Fig. 1. The 2-3 plane is the sample plane, and the 1 axis is perpendicular to the plane of the sample. The flat faces of the samples are painted with a silver electrode. The thickness and the diameter of each

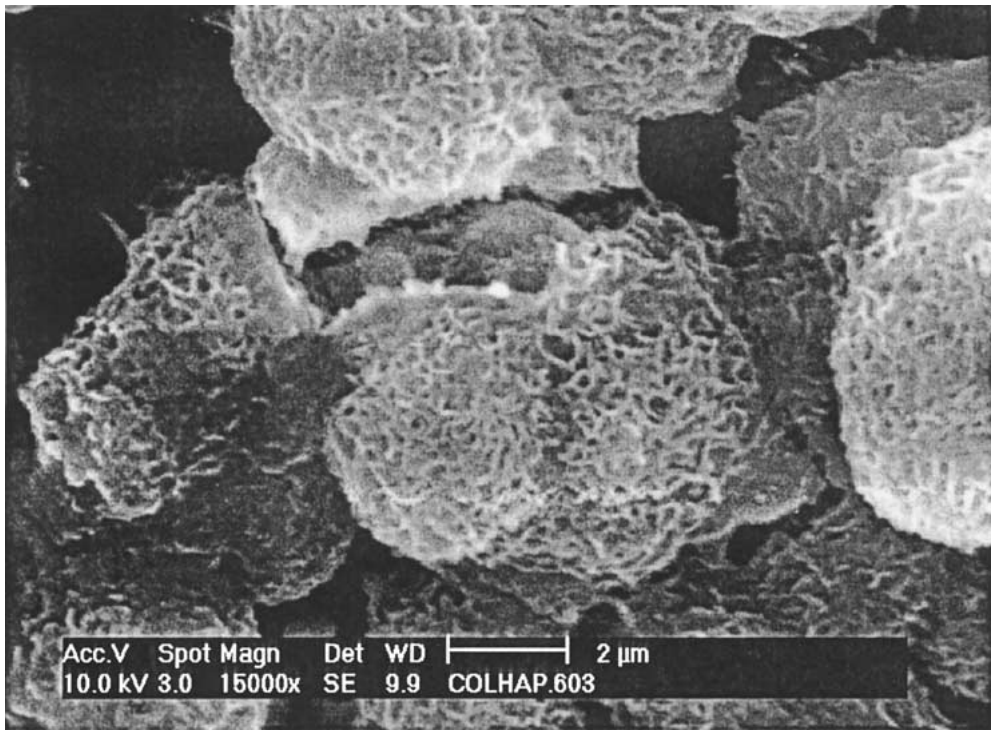

(E)

Figure 6 (*Continued*).

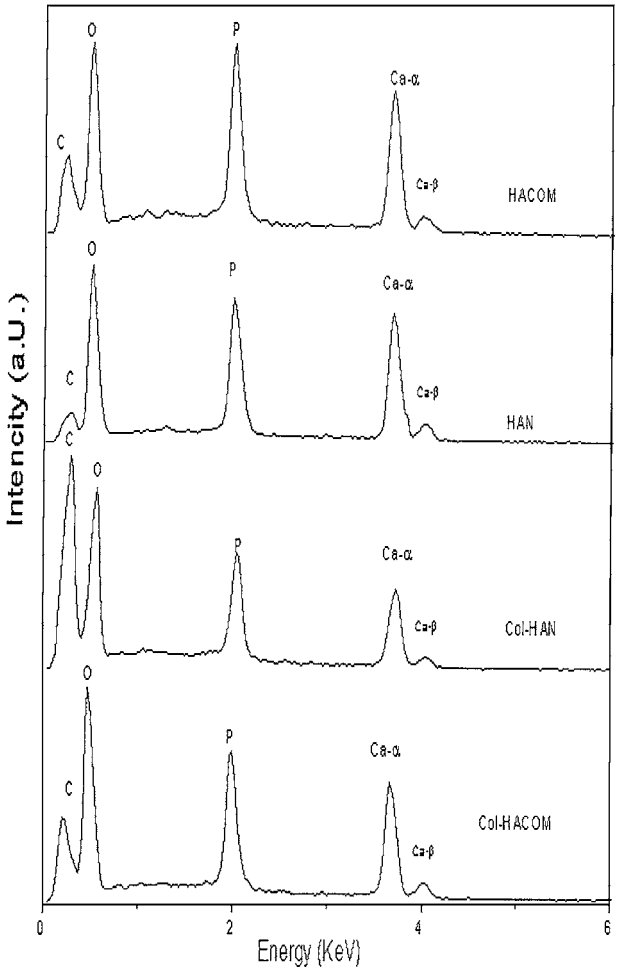

Figure 7 Energy Dispersive Spectroscopy in the collagen-HA composite samples: Col-HAN (Ca/P = 2.14), Col-HACOM (Ca/P = 1.71), HACOM powder (Ca/P = 2.38) and HAN powder (Ca/P = 2.07).

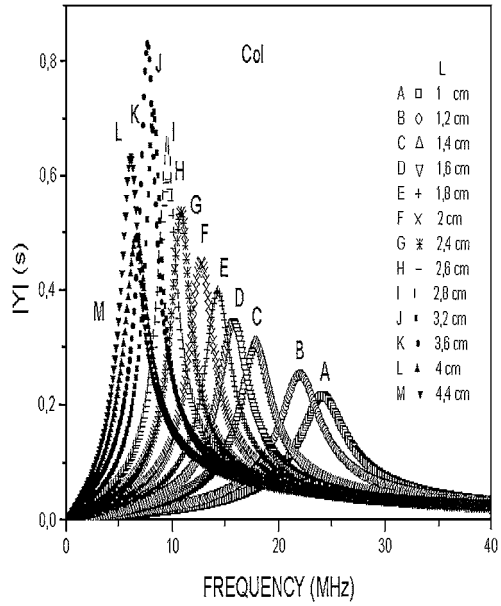

Figure 8 Electrical admittance as a function of external frequency and the disk diameter (L) for the anionic collagen film (Col).

sample are found in Table I and Figs 8–10. For all the studied samples the diameter 'L' was varied between 1, 0 cm to 4.4 cm, and the thickness 'e' was 27.88 μm, 150.72 μm and 97.68 μm for membranes of Col, Col-HACOM and Col-HAN respectively. In Fig. 8 one has the frequency dependence of the absolute value $|Y|$ of the admittance for anionic collagen film. The measurement was done with the sample in disk type geometry as shown in Fig. 1. In this figure, one has thirteen measurements for thirteen different diameters of the disk, which is indicated in the figure. From Fig. 8, the

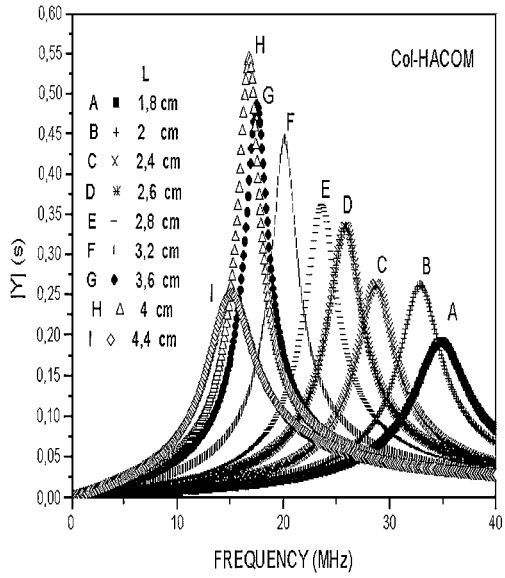

Figure 9 Electrical admittance as a function of external frequency and the disk diameter (L) for the collagen-HACOM composite film (Col-HACOM).

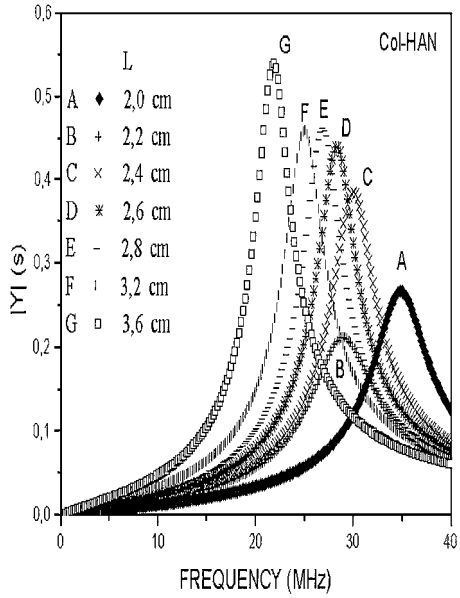

Figure 10 Electrical admittance as a function of external frequency and the disk diameter (L) for the collagen-HAN composite film (Col-HAN).

frequency constant, $f \cdot L$ associated to the piezoelectric mode of this sample was obtained. The average value obtained for the shear mode was $f \cdot L \sim 253.86$ kHz.m. In Figs 9 and 10 one has the admittance of composite film of Col-HACOM and Col-HAN respectively. We also did the measurement of the dielectric permittivity ε_{11}^T at 1 MHz, which is the dielectric permittivity obtained by a measurement of the capacitance at a frequency below the fundamental resonance, and ε_{11}^S at 1 GHz, which is the dielectric permittivity obtained by measurement of the capacitance at a frequency above the resonance mode, as we show in Table I. With the experimental measurements of ε_{11}, $f \cdot L$ and ρ and using Equations 1–3 one can obtain the piezoelectric strain element d_{14} for the piezoelectricity (see Table I). The piezoelectric strain tensor element d_{14} obtained for the anionic collagen was around 0.102 pC/N,

TABLE II Loss factor (Q^{-1}) for each sample as a function of the sample diameter (L)

		Col	Col-HACOM	Col-HAN
Q^{-1}	$L = 1.0$ cm	0.16	–	–
Q^{-1}	$L = 1.2$ cm	0.16	–	–
Q^{-1}	$L = 1.4$ cm	0.16	–	–
Q^{-1}	$L = 1.6$ cm	0.159	–	–
Q^{-1}	$L = 1.8$ cm	0.153	0.132	–
Q^{-1}	$L = 2$ cm	0.165	0.1	0.149
Q^{-1}	$L = 2.2$ cm	–	–	0.2
Q^{-1}	$L = 2.4$ cm	0.148	0.11	0.137
Q^{-1}	$L = 2.6$ cm	0.157	0.11	0.127
Q^{-1}	$L = 2.8$ cm	0.159	0.11	0.13
Q^{-1}	$L = 3.2$ cm	0.146	0.11	0.15
Q^{-1}	$L = 3.6$ cm	0.17	0.109	0.147
Q^{-1}	$L = 4$ cm	0.3	0.108	–
Q^{-1}	$L = 4.4$ cm	0.28	0.26	–

which is in good agreement compared with values reported in the literature obtained with other techniques [2, 8, 12]. In reference 15 collagen films were prepared by evaporation and electro-deposition from solution. It was observed that the electrodeposited films were more organized presenting higher piezoelectric coefficients than the evaporated films, with values around 0.076 pC/N. For the collagen-HA composite membranes a slight decrease of the value of the piezoelectricity was observed. However the collagen composite with nanocrystalline HA crystals (Col-HAN) present a better result ($d_{14} = 0.040$ pC/N, see Table I) compared to the composite with the commercial ceramic ($d_{14} = 0.012$ pC/N, see Table I). This is an indication that the nanometric particles of HA present little disturbance on the organization of the collagen fibers in the composite. In this situation the nanometric HA are the best candidates in future applications of these composites. From Table I one can see that Col-HAN composite films present the lowest density and highest value for the constant $f \cdot L$. We believe that high ionic force due to HA lead to a decrease of the self-organization (less anisotropy) of the microscopic fiber structure of the collagen, which could explain the slight decrease of the collagen-HA piezoelectricity. In Table II one has all the values of the loss factor Q^{-1} for all the samples. On average the Col and Col-HACOM samples present the higher and lower loss respectively, when compared to the other samples. In these measurements the collagen nanometric particles composite (Col-HAN) present an intermediate loss as expected. This is an indication that one can obtain higher piezoelectricity (d_{14}) and low loss using nanocrystalline HA for the composite samples.

5. Conclusions

In this paper we did a study of the physicochemical, dielectric and piezoelectric properties of anionic collagen and collagen-hydroxyapatite (HA) composites, considering the development of new biomaterials which have potential applications in support for cellular growth and in systems for bone regeneration. The piezoelectric strain tensor element d_{14}, the elastic constant s_{55}, and the dielectric permittivity ε_{11} were measured for

the anionic collagen and collagen-HA films. The X-ray diffraction pattern of the collagen film (Col) shows a broad band characteristic of an amorphous material. For the collagen-HA composite film (Col-HACOM) a high degree of crystallization was observed. The main peaks associated to the crystalline HA is present in sample of collagen-HACOM. For the nanocrystalline composite, nanometric HA powder (HAN), obtained by mechanical milling were used. According with the x-ray diffraction the average dimension of the HA grains is around 103 nm which were used to prepare our composite film (Col-HAN). For the composite film (Col-HAN) we have the diffraction intensities of the HA and $CaH(PO_4)_2$ H_2O phases. One can see that the HA powder (HAN) present the main peaks associated to crystalline HA.

The IR spectroscopy measurements on HA-COM and HAN powders, Col-HACOM and Col-HAN composite films and collagen film (Col) presents the main resonances associated to the modes of $(PO_4)^{3-}$ ion. Resonances associated to the stretching mode of the $(CO_3)^{2-}$ ion, were also observed at 876 cm^{-1}. The IR spectra of Collagen Film (Col) shows a strong absorption band associated to amide I (C=O), amide II (N–H) and a band centered at 1238 cm^{-1}, representing the amide III (C–N) vibrational modes. The spectrum of Col-HACOM composite sample is characterized by absorption bands arising from HA and Col, determined by analogy with FT-IR spectra of pure HA and Col standard samples.

The scanning electron photomicrography of the Col-HACOM and Col-HAN films, respectively, shows deposits of HA on the surface of collagen. It also shows that HACOM crystals has a dense feature, whereas the HAN crystals has soft porous surface. Energy-dispersive spectroscopy (EDS) analysis showed that the main elements of the hybrid sponge were carbon, oxygen, calcium, and phosphorus. The EDS of HACOM crystal, present in the Col-HACOM composite showed a molar ratio Ca/P = 1.71, whereas the Col-HAN composite the molar ratio of calcium and phosphorus (Ca/P = 2.14) and the amount of carbon were greater. The molar ratio obatained for the pure ceramics were 2.38 for HACOM ceramic and 2.07 for the nanocrystalline ceramic. These results suggest that the HAN crystals are closer to the expected value for the ratio Ca/P for hydroxyapoatite, which is around 2.15.

The piezoelectric strain tensor element d_{14} obtained for the anionic collagen was around 0.102 pC/N, which is in good agreement compared with values reported in the literature obtained with other techniques. The collagen composite with nanocrystalline HA crystals (Col-HAN) present a better result ($d_{14} = 0.040$ pC/N) compared to the composite with the commercial ceramic ($d_{14} = 0.012$ pC/N). This is an indication that the nanometric particles of HA present little disturbance on the organization of the collagen fibers in the composite. In this situation the nanometric HA are the best candidates in future applications of these composites. The Col-HAN composite films present the lowest density and highest value for the constant $f \cdot L$. We believe that high ionic force due to HA lead to a decrease of the self-organization (less anisotropy) of the microscopic fiber structure of the collagen, which could explain the slight decrease of the collage-HA piezoelectricity. On average the Col and Col-HACOM samples present the higher and lower loss respectively, when compared to the other samples. In these measurements the collagen nanometric particles composite (Col-HAN) present an intermediate loss as expected. This is an indication that one can obtain higher piezoelectricity (d_{14}) and low loss using nanocrystalline HA for the composite samples.

Acknowledgements

This work was partly sponsored by FINEP, CNPq (Brazilian agencies). The authors also acknowledge P. L. Sombra for the help with the draw of the experimental setup.

References

1. L. L. HENCH, *J. Amer. Ceram. Soc.* **81**(7) (1998) 1705.
2. S. RHEE and J. TANAKA, *ibid.* **81**(11) (1998) 3029.
3. Y. DOI, T. HORIGUCHI, Y. MORIWAKI, H. KITAGO, T. KAJIMOTO and Y. IWAYAMA, *Journal of Biomedical Materials Research* **31** (1996) 43.
4. A. BIGI, S. PANZAVOLTA and N. ROVERI, *Biomaterials* **19** (1998) 739.
5. Q. LIU, J. R. DE WIJN and C. A. VAN BLITTERSWIJK, *Journal of Biomedical Materials Research* **40**(2) (1998) 257.
6. M. E. NIMNI, "Collagen: Biochemistry," Vol. 1 (CRC, 1988).
7. *Idem.*, "Collagen: Biotechnology," Vol. 3 (CRC, 1988).
8. K. E. KADLER, D. F. HOMES and J. A. CHAPMAN, *Biochem. J.* **316** (1996) 1.
9. J. A. CHAPMAN, *Electron Microsc. Rev*. **3** (1990) 143.
10. G. M. SESSLER (ed.), "Electrets, Topics in Applied Physics," Vol. 23, Electrets (Springer-Verlag, Berlin, 1980) p. 321.
11. H. S. NALWA (ed.), "Ferroelectric Polymers" (Marcel Dekker Inc., 1995) p. 393.
12. G. W. HASTNIGS and F. A. MAHMUD, *J. Biomed. Eng.* **10** (1988) 515.
13. F. JIANQING, Y. HUIPIN and Z. XINGDONG, *Biomaterials.* **18** (1997) 1531.
14. J. B. PARK and R. S. LAKES, "Biomaterials: An Introduction" (Plenum Press, NY, 1992).
15. A. A. MARINO *et al.*, *Calcif. Tissue Int.* **31** (1980) p. 257.
16. *J. Phys. and Chemistry of Solids*, submitted; *J. Mater. Science*, submitted.
17. C. C. SILVA, A. G. PINHEIRO, D. THOMAZINI, J. C. GÓES, S. D. FIGUEIRÓ, J. A. C. DE PAIVA and A. S. B. SOMBRA, *Materials Science and Engineering* B **83** (2001) 165.
18. L. V. AZÁROFF, "Elements of X-ray Crystallography" (McGraw-Hill Book Company, New York, 1968).
19. T. IKEDA, "Fundamentals of Piezoelectricity" (Oxford Sci., 1996).
20. *Idem.*, *J. Phy. Soc. Japan* **13** (1958) 809.
21. A. VEIS, "The Macromolecular Chemistry of Gelatin" (Academic Press, 1964).
22. G. GOISSIS, E. M. JUNIOR, J. A. C. MARCANTONIO, R. C. C. LIA, D. C. J. CANCIAN and M. DE CARVALHO, *Biomaterials* **20**(1) (1999) 27.
23. G. GOISSIS, L. PICCIRILI, J. C. GOES, A. M. D. PLEPIS and D. K. DAS-GUPTA, *Artificial Organs* **22**(3) (1998) 203.
24. Joint Committee on Powder Diffraction Standards (JCPDS), International Center for Diffraction Data, 12 Campus Blvd., Newton Square, Pennsylvania 19073–3723, USA, 1995.
25. P. L. GORDON, I. V. YANNAS, J. F. BURUKE and R. C. LORD, *Macromolecules* **7** (1974) 954.
26. G. N. RAMACHANDRAN, "Treatise on Collagen," Vol. 1 (Academic Press, London, 1967).
27. A. COOPER, *Biochem. J.* **118** (1970) 353.
28. D. G. WALLACE, *Biopolymers* **29** (1990) 1015.

Received 1 March
and accepted 21 December 2001